Accident Analysis and Prevention 178 (2022) 106834

Contents lists available at ScienceDirect

Accident Analysis and Prevention

journal homepage: www.elsevier.com/locate/aap

Developing an improved automatic preventive braking system based on safety-critical car-following events from naturalistic driving study data

Weixuan Zhou [a,b], Xuesong Wang [a,b,*], Yi Glaser [c], Xiangbin Wu [d], Xiaoyan Xu [a,b]

[a] School of Transportation Engineering, Tongji University, Shanghai 201804, China
[b] The Key Laboratory of Road and Traffic Engineering, Ministry of Education, Shanghai 201804, China
[c] Global Safety Center, GM, Warren, MI 48092-2031, USA
[d] Intelligent Driving Lab, Intel Labs China, Beijing 100190, China

ARTICLE INFO

Keywords:
Automatic preventive braking
Autonomous emergency braking
Car-following scenario
Naturalistic driving study
Safety-critical event

ABSTRACT

In public road tests of autonomous vehicles in California, rear-end crashes have been the most common type of crash. Collision avoidance systems, such as autonomous emergency braking (AEB), have provided an effective way for autonomous vehicles to avoid collisions with the lead vehicle, but to avert false alarms, AEB tends to apply late and hard brake only if a collision becomes unavoidable. Automatic preventive braking (APB) is a new collision avoidance method used in Mobileye's Responsibility-Sensitive Safety (RSS) model that aims to reduce crashes with a milder brake and decreased impact on traffic flow, but APB's safety performance is inferior to that of AEB. This study therefore proposes three safety improvement strategies for APB, the addition of response time, safety buffer, and minimum following distance; and combines them in different ways into four improved APB systems, IP1-IP4. Simulating car-following safety–critical events (SCEs) extracted from the Shanghai Naturalistic Driving Study in MATLAB's Simulink, the safety performance, conservativeness, and driving comfort of the four systems were evaluated and compared with the original APB system, two AEB systems, and human drivers. The results show that 1) IP4, the system that integrated all three strategies, outperformed the baseline APB and IP1-IP3 and prevented all SCEs from becoming crashes; 2) IP4 was slightly more conservative than AEB, but less conservative than RSS; 3) APB's jerk-bounded braking profile improved driving comfort; and 4) higher deceleration was found in the two AEB systems (both 8.1 m/s^2) than in IP4 (6.7 m/s^2), but they failed to prevent all crashes. Our proposed APB system, IP4, can provide safe, efficient, and comfortable braking for AVs in car-following SCEs, and has the potential to be practically applied in vehicle collision avoidance systems.

1. Introduction

The new emerging autonomous vehicle (AV) has a promising future due to its potential for solving current transportation issues, such as traffic safety and congestion. In the transition period before all vehicles are autonomous, however, AVs and human-driven conventional vehicles will coexist for a long period of low AV penetration, and this period of mixed traffic will bring enormous challenges for AVs, such as high collision risk and low traffic stability (Zhang and Gao, 2020). As more than half of the AV crashes in California public road testing were rear-end crashes (Liu et al., 2021a, Liu et al., 2021b; Xu et al., 2019), avoiding rear-end collisions is one of the AV's main challenges.

The autonomous emergency braking (AEB) system is a collision avoidance system designed to help drivers avoid or mitigate the severity of rear-end crashes. AEB is a subset of the Forward Crash Avoidance and Mitigation (FCAM) systems investigated by the National Highway Traffic Safety Administration (NHTSA, 2014). With front radar and camera detecting position and velocity of surrounding objects, AEB can work with forward collision warning (FCW) to alert drivers of potential risk, and automatically apply brake support or emergency braking when the vehicle is on the verge of collision. Due to the systems' safety benefits in avoiding collisions and reducing speed when collisions cannot be avoided (Fildes et al., 2015; Kusano and Gabler, 2012), the European Commission, United States, and others have issued laws and regulations requiring the installation of AEB and FCW in new cars and trucks. A collision avoidance system includes three main subsystems: environment sensing, decision-making, and execution (Yang et al., 2022). Decision-making is the core component of a collision avoidance system,

* Corresponding author at: School of Transportation Engineering, Tongji University, Shanghai 201804, China.
E-mail address: wangxs@tongji.edu.cn (X. Wang).

https://doi.org/10.1016/j.aap.2022.106834
Received 23 December 2021; Received in revised form 25 August 2022; Accepted 10 September 2022
Available online 21 September 2022

which decides when and how to react based on safety criteria such as time-to-collision (TTC). In decision-making, the trade-off between false alarms (false positive) and missed detections (false negative) is always of concern. To reduce the false alarm rate, the AEB tends to delay brake activation until a crash is imminent, that is, it waits for a short TTC, after which it brakes with high deceleration (usually 0.8 g to 1.0 g) (Lee and Peng, 2005; Doecke et al., 2012; Coelingh et al., 2010). Even so, not all crashes can be prevented, moreover, sudden braking with high deceleration is likely to affect the driver's comfort and increases the collision risk with an unprepared following vehicle.

Automatic preventive braking (APB) is another collision avoidance system. Using a safe distance criterion for brake activation, it aims to reduce crashes without compromising traffic efficiency or driving comfort by applying a mild brake early (Shalev-Shwartz et al., 2018). APB originated in Mobileye's Responsibility-Sensitive Safety (RSS) model (Shalev-Shwartz et al., 2017), a model that has been demonstrated to provide safety assurance in safety–critical car-following and cut-in scenarios (Xu et al., 2021; Liu et al., 2021a, Liu et al., 2021b), and that has been applied in the autonomous driving strategies of Baidu Apollo and Mobileye as a safety guarantee. Yet despite its safety assurance, RSS is considered by some studies as overly conservative and wasteful of road resources (Zhao et al., 2019; Li et al., 2018). APB does not show the same level of safety when tested with real traffic data. Zhou and Wang (2022) evaluated APB's performance and found that APB does have better driving stability than AEB, but is more likely to cause crashes, possibly because its deceleration is easily affected by its changing kinetic parameters. The same study also found that APB's distance-triggered braking was more sensitive and adjustable than the AEB's TTC-triggered braking, indicating that APB has more potential for safety improvement.

APB's proactive milder and earlier braking has greater capacity for increasing AV passenger comfort and reducing impact on traffic flow, while its safety issues suggest specific modifications that can be made. Specifically, APB does not consider response time, its safe distance fluctuates, and it is less effective in low-speed close car-following scenarios such as traffic jams. By making and testing suitable modifications, this study aims to improve the safety performance of APB in relation to the lead vehicle, as well as determine whether it can do so without sacrificing driver and passenger comfort, and without being as conservative as RSS.

Collision avoidance systems such as AEB can be field tested in scenarios with testing protocol configurations released by organizations such as NHTSA, the European New Car Assessment Programme, and the Insurance Institute for Highway Safety, but such collision tests are costly and impractical for testing systems such as APB that are in their initial stages of development. Virtual tests with real traffic data are low cost, easy to repeat, and enable detailed analysis of the collision process. Previous studies, for example, have used in-depth accident data to simulate pre-crash scenarios to estimate AEB's benefit in terms of number of collisions mitigated or eliminated (Char et al., 2022; Jeppsson and Lubbe, 2020). However, crashes are rare events and difficult to collect. Advanced data collection technologies such as the naturalistic driving study (NDS) have enabled the observation of safety–critical event (SCEs), which entails circumstances that require rapid evasive maneuvers by the road user and may end with either a crash or near-crash. Guo (2019) found that drivers are ten times more likely to encounter near-crashes than crashes, indicating that SCEs provide a more feasible approach to safety research. More importantly, autonomous braking systems should help to defuse the risk of near-crashes becoming crashes, but the benefit of braking systems in preventing near-crashes from deteriorating into crashes has not been tested.

The main objective of this study is to develop an improved APB system and compare it with selected AEB systems. The proposed system is designed to apply an appropriate deceleration profile to reduce rear-end collisions without compromising driving stability or efficiency; it is designed to deal with the three mentioned safety issues of the original APB by making modifications to response time, safety buffer, and minimum following distance. The APB and AEB systems are tested in this study with real-life car-following SCEs extracted from the Shanghai NDS.

2. Literature review

2.1. Safety-Critical events (SCEs)

In the 100-Car NDS, the first of its kind, safety events were classified according to their severity as crash, near-crash, crash-relevant conflict, and proximity conflict. Near-crashes involve circumstances that require rapid evasive maneuvers by the subject vehicle, or any other vehicle, pedestrian, cyclist, or animal, to avoid a crash (Dingus et al., 2006). Near-crashes are commonly used as a surrogate measure of crashes, as previous studies have found that a positive relationship exists between crashes and near-crashes (Guo et al., 2010), and that the number of near-crashes can be used to predict crash frequency by both logit and probit models (Wu and Jovanis, 2012). The causal mechanisms of crashes and near-crashes have been demonstrated as similar, the major difference between them being the severity of the event (Guo et al., 2010) as well as the activation time and intensity of the evasive maneuvers.

The extraction of SCEs, which in the current paper include crashes and near-crashes, usually aims to identify rapid evasive maneuvers including steering, braking, accelerating, or any combination of these maneuvers. In the 100-Car NDS, drivers performed rapid braking maneuvers in more than 80 % of SCEs (Dingus et al., 2006); a large longitudinal deceleration (e.g., a minimum of 0.5 g as is shown in Table 1) is an effective indicator of an SCE, as is a smaller deceleration coupled with a short forward time-to-collision (TTC). A rapid steering maneuver is characterized by a large lateral acceleration in either direction, shown in Table 1 as being triggered in the various studies as 0.55 g at the least, or by a rapid change in travel direction within a short time window, triggered by a change in yaw rate of a minimum of 4 deg in 3 s. SCEs are typically identified from raw NDS data with a two-step process: 1) set a series of criteria and automatically filter the kinematic data to extract the candidate events; 2) manually validate the front videos of the candidate events to remove invalid events. The criteria used in previous studies are summarized in Table 1, which, in addition to the lateral and longitudinal criteria just mentioned, include the driver's activation of the NDS dashboard event button.

2.2. Autonomous emergency braking (AEB)

AEB systems that have been tested and are currently in the marketplace can be classified into at least three categories: 1) one-stage AEB activated by a time-related trigger such as TTC or a distance-related trigger such as safe braking distance, 2) AEB combined with forward collision warning (FCW), and 3) multi-stage AEB with or without FCW (Kusano and Gabler, 2012; ADAC, 2013; Cicchino, 2016). The most fundamental and commonly used collision avoidance pattern is one-stage AEB activated by TTC (Park et al., 2017). In this AEB system, when the TTC drops below a pre-defined value (usually between 0.5 s and 1.5 s), the vehicle automatically performs an emergency braking maneuver. The addition of multiple stages and FCW is intended to best assist drivers by giving them enough time to perform a proper evasive maneuver, and then to provide full brake when a crash becomes otherwise unavoidable (ADAC, 2013). Some manufacturers such as Audi, Volvo, and Volkswagen combine FCW with multi-stage partial and fully autonomous braking together. The three-stage AEB used in the Audi A7 has been tested and shown to perform well (ADAC, 2013), as has the basic and commonly used one-stage AEB. This study will therefore compare the performance of these two AEB systems with APB in car-following SCEs.

Table 1
Summary of trigger criteria used in existing literature.

Author	Lateral acceleration (g)	Longitudinal acceleration (g)	Event button	Longitudinal acceleration (g) & forward TTC (s)		Yaw rate (deg/s)
				Longitudinal acceleration	Forward TTC	
Dingus et al. (2006)	≥ 0.7*	≥ 0.6*	Activated	≤ -0.5	≤ 4	$\geq \pm 4$ deg in 3 s
Lee et al. (2011)	≥ 0.75*	≥ 0.65*	Activated	≤ -0.65	≤ 4	$\geq \pm 4$ deg in 3 s
Hankey et al. (2016)	≥ 0.75*	≤ -0.65	Activated	/	/	$\geq \pm 8$ deg in 0.75 s
Perez et al. (2017)	≥ 0.92*	≤ -0.75	Activated for more than 0.74 s	/	/	$\geq \pm 8$ deg in 75 s
Carney et al. (2010)	≥ 0.55*	≤ -0.50	/	/	/	/

Note: * indicates absolute value of acceleration.

2.3. Automatic Preventive braking (APB)

APB is activated by a safe distance criterion. Safe distance (stopping distance, or braking distance) is the minimum distance that the lead and following vehicle should keep between them considering their current speed and acceleration under a hypothetical deceleration and desired reaction time (Lee et al. 2014). Several main types of safe distance algorithms include Mazda's algorithm (Doi et al., 1994), Honda's algorithm (Fujita et al., 1995), the NHTSA alert algorithm (Burgett et al., 2001), and the Berkley algorithm (Seiler et al., 1998). The safety performance and conservativeness of these algorithms vary due to their different assumptions regarding vehicle braking pattern, system delay, and response time.

APB adopts a jerk-bounded braking profile that is different from the aforementioned algorithms (and will be further described in Section 4.3) and has aroused the interest of researchers (Gassmann et al., 2019; Koopman and Osyk, 2019). Mattas et al. (2020) tested APB in rear-end collisions and found that including jerk made the safe distance calculation more accurate. Zhou and Wang (2022) discovered that APB's braking process fluctuates frequently, which will erode the reserved braking distance and increase the possibility of a crash. In RSS and other collision avoidance models (Chen et al., 2013; Brannstrom et al., 2008) that calculate safe distance, the distance that the AV travels during its response time is usually considered. Response time, however, is not considered in the current APB model, which may lead to a short safe distance and inadequate braking distance. Standstill distance which is always considered in car-following models (Cunto and Saccomanno, 2008; Treiber et al., 2000) to maintain the minimum following distance is also not considered in APB. These issues may increase the probability of crashes and should be carefully considered in the improvement of APB system.

3. Data preparation

3.1. Extraction of Safety-Critical events

The Shanghai Naturalistic Driving Study (SH-NDS) was the first NDS in China. The three-year data collection that started in December 2012 and ended in December 2015 was conducted collaboratively by Tongji University, General Motors, and the Virginia Tech Transportation Institute. Five testing cars, or subject vehicles (SV), were equipped with advanced data acquisition systems (DAS), including four cameras (facing front, rear, driver's hands, and driver's face), radar, GPS, speedometer, three-dimensional accelerometer, and the Mobileye C2-270 Collision Prevention System (Mobileye, 2010). Each recruited driver was allowed to keep and drive a testing car for two months without any intervention. There was no limitation of travel area, but as the drivers were recruited in Shanghai, the vast majority of the naturalistic driving data was collected in Shanghai. A total of 19,133 trips were recorded, with 161,055 total kilometers driven. The five SVs functioned in the current study as following vehicles traveling behind lead vehicles (LVs).

With the rich kinematic data and video data obtained from the NDS's real-life driving, safety–critical events (SCEs) were extracted for this study. Candidate events with high longitudinal and lateral acceleration and low TTC were extracted with a series of criteria. The criteria were initially set according to the 100-car Naturalistic Study (Dingus et al. 2006) and SHRP2 (Hankey et al., 2016), and slightly adjusted so as to balance the false positive and false negative rates (Wang and Xu, 2019). If any of the following criteria were met, the event was tagged as a candidate SCE.

- Trigger 1: Longitudinal acceleration less than or equal to −0.5 g;
- Trigger 2: Lateral motion equal to or greater than 0.7 g;
- Trigger 3: Event button activated by the driver by pressing a button on the dashboard when an event occurred that he/she deemed critical;
- Trigger 4: Lateral motion equal to or greater than 0.5 g coupled with a forward TTC less than or equal to 4 s;
- Trigger 5: Longitudinal acceleration less than or equal to −0.45 g coupled with forward TTC less than or equal to 4 s.

Application of the initial criteria resulted in the extraction of 3,623 potential SCEs. By manually validating the videos to ensure that in each event the following SV had to perform an evasive maneuver to prevent collision with the LV, 249 car-following SCEs were extracted.

3.2. Analysis of the extracted events

Each of the 249 events was then analyzed for a 15-second period from 5 s prior to and 10 s after the trigger moment. Twenty-six of the 249 SCEs were omitted as the sensor lost the LV for more than 10 s, making it impossible to track the continuous trajectory of the LV. The remaining 223 SCEs included one crash.

Fig. 1 illustrates the distributions of the main parameters of the 223 SCEs in the form of histograms, with cumulative distributions indicated by the red lines. Nearly 90 % of the SCEs start with a relative distance shorter than 20 m, as is shown in Fig. 1a. The average minimum TTC was 1.31 s, with nearly 70 % of the SCEs having a minimum TTC lower than 1.5 s (Fig. 1b), substantially lower than the TTC thresholds dividing safe and dangerous situations in most previous research: 4 s (Hirst and Graham, 1997), 3 s (Minderhoud and Bovy, 2001), and 2.6 s (Hogema and Janssen, 1996). According to Gettman et al. (2008) who used a threshold of 1.5 s, most of the events in this study should be considered "severe." The average LV maximum deceleration was 0.66 g in Fig. 1c; the average SV maximum deceleration and maximum jerk (the first derivative of acceleration) were 0.62 g (Fig. 1e) and 2.06 g/s (Fig. 1f) respectively. Together, these averages indicate that in most SCEs, the LVs applied sharp brakes and the SVs also braked hard to avoid potential rear-end collisions.

As the 223 SCEs would be handled in this study by APB, one-stage AEB, and three-stage AEB systems, it was essential to extract from the data the key parameters for these systems. The 50th, 75th, and 95th

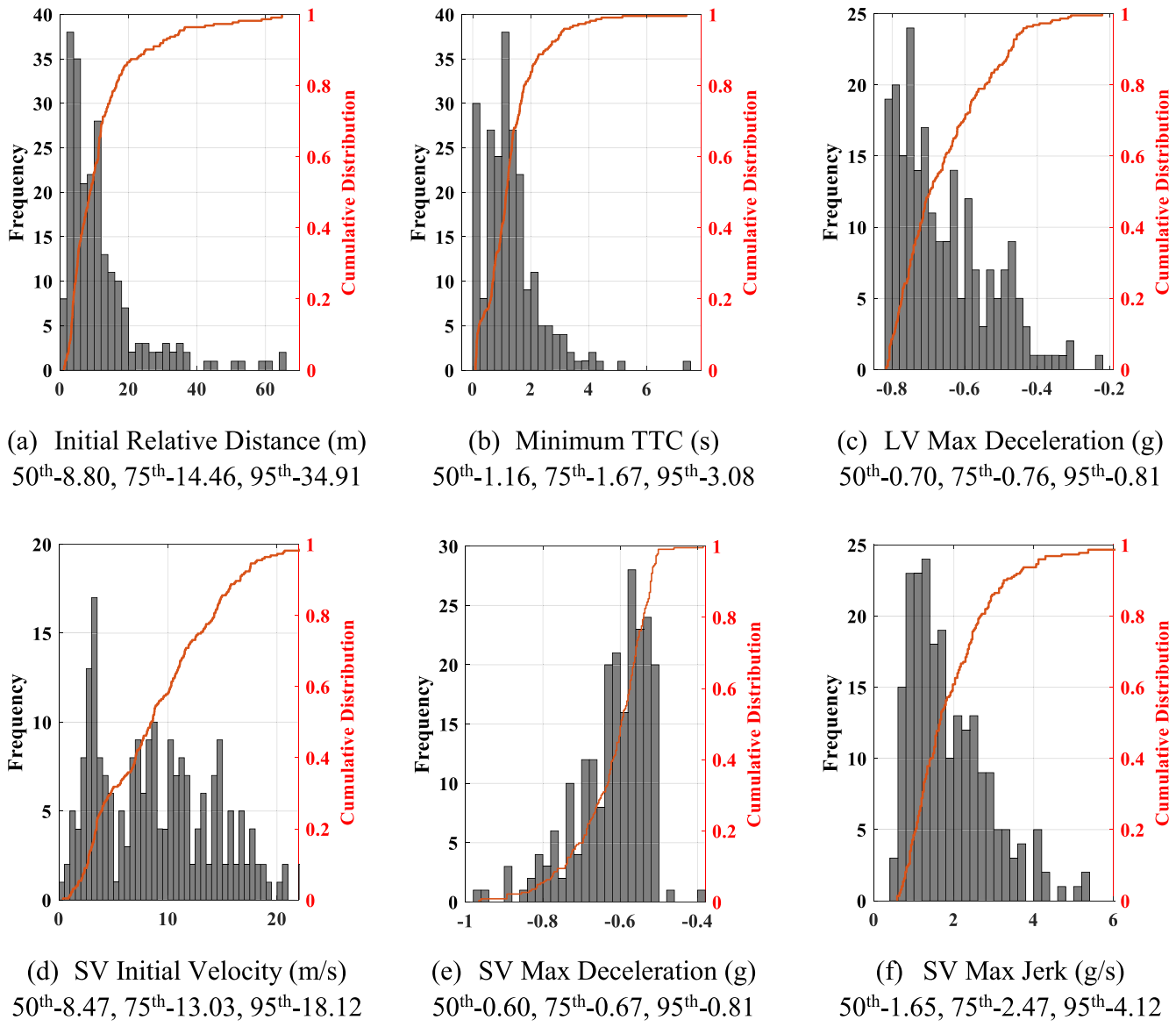

Fig. 1. Distribution and 50th, 75th, and 95th Percentiles of Main SCE Parameters.

percentiles of SV max deceleration (1e), SV max jerk (1f), LV max deceleration (1c), and SV initial velocity (1d) will be used to determine the parameter values of APB, one-stage AEB and three-stage AEB systems in the following correspondence, and will be detailed explained in Section 4.

- $a_{min,brake}$ of APB: SV max deceleration
- $a_{max,brake}$ of APB: LV max deceleration
- j_{max} of APB: SV max jerk
- Deceleration of one-stage AEB: SV max deceleration
- TTC threshold of one-stage AEB: SV initial velocity and SV max deceleration
- Deceleration of three-stage AEB: SV max deceleration

3.3. Generation of Safety-Critical scenarios

To rebuild the SCEs into scenarios in the simulator, the kinetic parameters recorded by the SVs were extracted from the NDS data: the SV velocity, the relative distance of the SV and LV, and their relative velocity. These parameters were then used to generate the LVs' velocities and trajectories.

The scenario generating process can be divided into two steps (Fig. 2). In step 1, the LV's longitudinal and lateral velocity at each simulation step i was derived from the SV's velocity and the relative velocity between the vehicles. In step 2, the LV's trajectory was derived from its own velocity by the following equation:

$$P_i^x = \begin{cases} P_{i-1}^x + v_i^x \times \Delta t, & i \geqslant 2 \\ \Delta r_1^x, & i = 1 \end{cases}$$
$$P_i^y = \begin{cases} P_{i-1}^y + v_i^y \times \Delta t, & i \geqslant 2 \\ \Delta r_1^y, & i = 1 \end{cases} \quad (1)$$

where P_i^x (P_i^y) and v_i^x (v_i^y) denote the longitudinal (lateral) position and velocity of the LV at time i; Δt denotes the simulation step length, which is 0.1 s in this study; and Δr_1^x and Δr_1^y are the initial relative distances between the two vehicles. The initial position of the SV was set as (0,0) in the simulation, so the initial position of the LV should be the initial relative distance between the two vehicles.

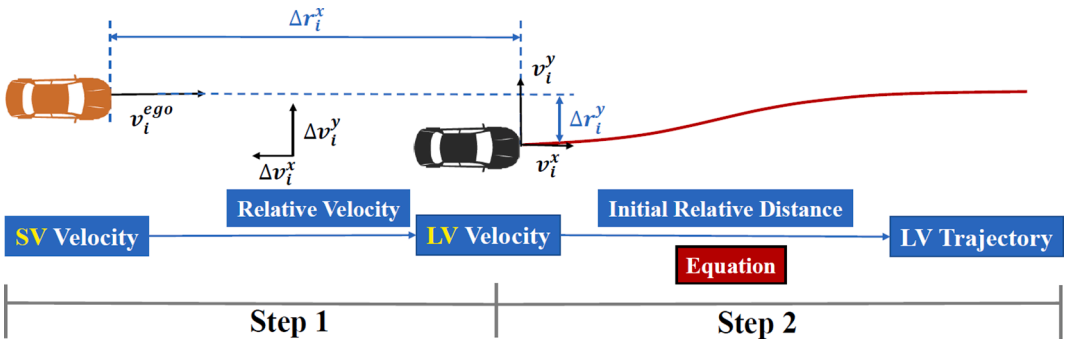

Fig. 2. Generating LV Velocity and Trajectory.

4. Methodology

4.1. Simulation platform

This study used the MATLAB Automatic Driving Toolbox to create and virtualize the driving scenarios and to simulate driving behavior under the AEB and APB systems. MATLAB's Driving Scenario Designer app was used to create the test scenario for every SCE, including the road's center and width, the LV's trajectory and velocity, and the initial velocity and position of the SV, now the simulated AV, or ego car. The LV's trajectory and velocity were generated by the pre-processing procedure in Section 3.3, the AV's initial velocity was its real initial velocity taken from the SCE, and its initial position was the origin of the coordinates. The road center was set as a straight line as vehicles were found to drive approximately straight in the NDS car-following SCEs, and road boundaries were automatically inferred by the toolbox. In order to focus on the interaction between the LV and the AV rather than environmental factors, conditions such as weather were not simulated.

The simulation was realized by the collaboration of two subsystems consisting of four blocks. Fig. 3 illustrates the blocks designed in Simulink to test the AEB system. The APB system uses the same simulation structure, simply replacing the AEB controller with the APB controller.

In the AEB with Sensor Fusion subsystem, the *tracking and sensor fusion* block fuses the data from the sensors and detects the most important object (MIO), as well as its position and velocity. The *AEB and speed controller* decides the driving strategy of the next simulation step by analyzing the current safety condition, and outputs the brake pressure or throttle to the Vehicle and Environment subsystem. The *vehicle dynamics and driver steering model* block models the dynamics of the simulated ego car as it drives along the road. The motion of the ego car is synchronized in the scenario by the *actors and sensor simulation* block, after which the sensors output the data for the next step in the simulation. The simulation was run once for each scenario for each of the braking algorithms under study, as the simulation result does not change with simulation times.

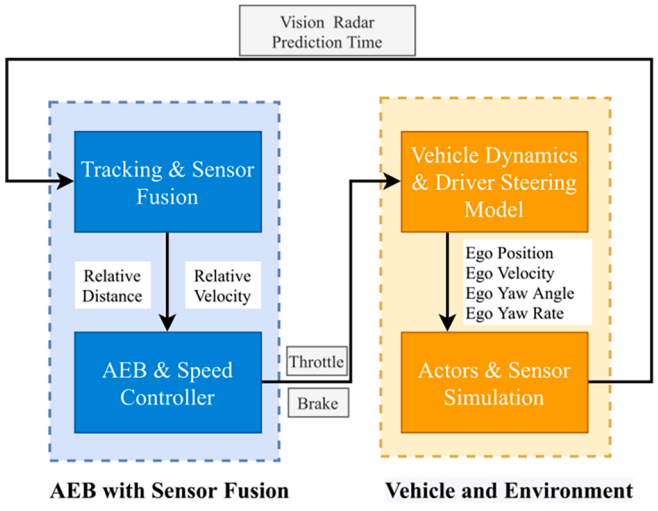

Fig. 3. AEB Simulation Procedure in Simulink.

4.2. AEB systems

Two different AEB systems, a one-stage AEB and a three-stage AEB, were studied for comparison with the APB. Fig. 4 shows the braking profiles of the three systems. In the one-stage AEB, the vehicle brakes with a constant deceleration d_{one} when the TTC becomes shorter than the threshold TTC_b. In the simulation, the ego vehicle is designed to drive at its initial velocity until it brakes with d_{one}, so the time that it requires to achieve a full brake is its initial velocity divided by d_{one}, namely TTC_b. The values used for d_{one} and initial velocity are approximations of the 50th, 75th, 95th percentiles of the SV's maximum deceleration and initial velocity parameters in Fig. 1. Nine (3×3) one-stage AEB algorithms were pre-tested, and as the results showed that the algorithm with $d_{one} = 8.1\ \mathrm{m/s^2}$ and $TTC_b = 2.22$ s had the least number of crashes, it was chosen for further study.

The second AEB system chosen for comparison was a three-stage cascaded AEB with early forward collision warning (FCW). The system utilizes the stopping time calculation approach that continuously compares current TTC with stopping time. Stopping time (τ_{stop}) is the time from when the ego vehicle first applies its brake a_{brake} to the time it comes to a complete stop when travelling at the velocity of v_{ego} (Eq. (2)).

$$\tau_{stop} = \frac{v_{ego}}{a_{brake}} \tag{2}$$

As is shown in Fig. 4, T_{FCW} is the stopping time, assuming the driver brakes at $4\,\mathrm{m/s^2}$ after a reaction time of 1.2 s at current speed. If the driver fails to respond to the warning by applying the brake in time, the AEB will be activated. The brake pressure of the first stage is $d^1_{three} = 4\,m/s^2$, which is set lower than the SV's maximum deceleration in the NDS data so that a softer brake can be applied when the condition is less critical. The second stage and third (full brake pressure) stage refer to the 75th percentile ($d^2_{three} = 6.7\,m/s^2$) and 95th percentile ($d^3_{three} = 8.1\,m/s^2$) of SV maximum deceleration, respectively. The stopping time at each braking stage is calculated as T_{stop1}, T_{stop2} and T_{stop3}, whereupon if TTC is shorter than stopping time, brake pressure is applied.

4.3. APB system

As mentioned earlier, the APB originated in the RSS, so the decision-making and control procedures of the two algorithms are similar: as is shown in Fig. 4, in a car-following situation, the ego car (or the SV in the NDS) continuously compares its relative distance to the LV with the safe distance, which is the difference in distance that each of the two vehicles requires to reach a full stop. When relative distance is smaller than safe

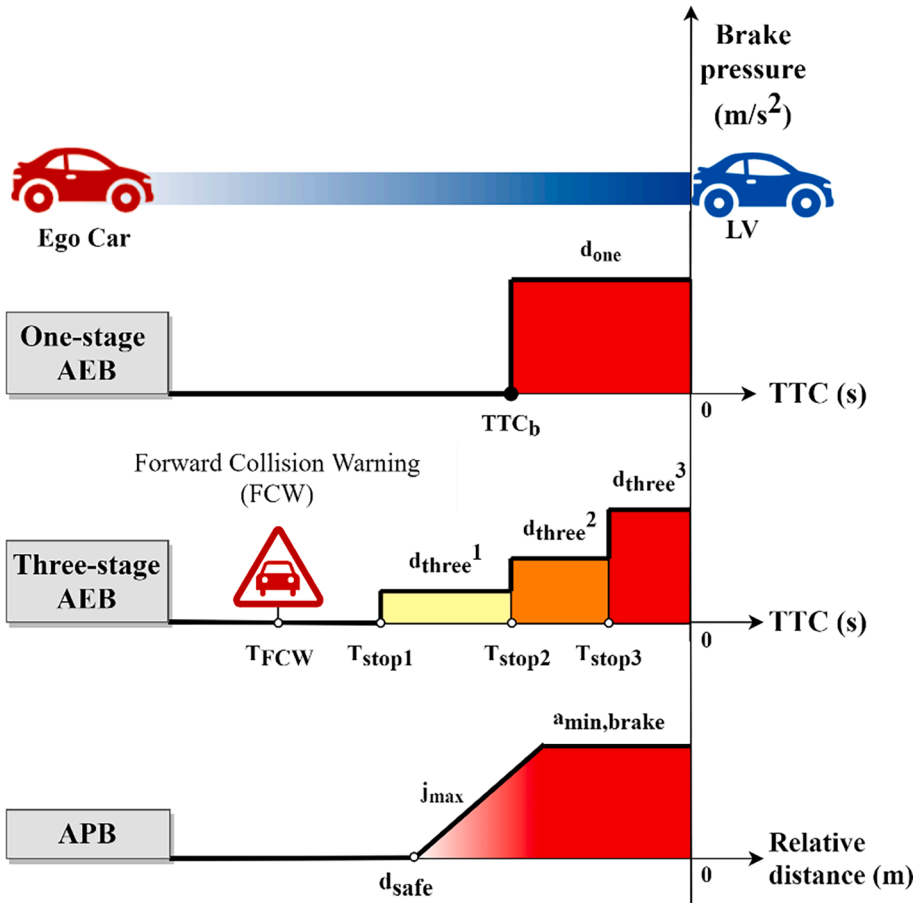

Fig. 4. Braking profiles of one-stage AEB, three-stage AEB, and APB systems. The filled dot on the one-stage AEB x-axis (at point TTC_b) indicates a fixed threshold while the open dots for the other systems (e.g., at T_{stop1}) indicate thresholds that vary with real-time parameters, e.g. speed and acceleration.

distance, the ego car enters an unsafe driving condition so it will decelerate until it stops or the distance becomes safe. To make the braking gentler, APB redefined the longitudinal safe distance by substituting the original braking profile of the following vehicle with a jerk-bounded profile (Eq. (3)). That is, instead of braking with a minimum reasonable braking value $a_{min,brake}$, the vehicle brakes with a constant jerk j_{max} until it reaches the $a_{min,brake}$. The notations for Equations (3) to (8) are explained in Table 2.

$$a(t) = \begin{cases} a_0 - j_{\max} t, & a(t) < a_{\min,brake} \\ a_{\min,brake}, & else \end{cases} \tag{3}$$

Based on the jerk-bounded profile, the braking distance is defined as follows:

Table 2
APB functions.

Notation	Explanation
a_0	Initial acceleration of the ego vehicle.
v_0	Initial velocity of the ego vehicle.
v_f	Velocity of the lead vehicle
$a_{\min,brake}$	Minimum reasonable braking value for the ego vehicle
$j_{\max}$	Maximum jerk for the ego vehicle
$a_{\max,brake}$	Maximum possible braking value of the lead vehicle
T_1	Time when acceleration reaches $a_{\min,brake}$
T_2	Time when ego velocity reaches 0
T	Minimum value of T_1 and T_2
d_{brake}	Distance the ego vehicle travels before reaching a full brake
d_{safe}	Safe distance
$d_{relative}$	Relative distance between ego and lead vehicle
ρ	Response time of ego vehicle

$$d_{brake} = [v_0 T + \frac{1}{2} a_0 T^2 - \frac{1}{6} j_{\max} T^3] + \frac{(v_0 + a_0 T - \frac{1}{2} j_{\max} T^2)^2}{2 a_{\min,brake}} \tag{4}$$

where T is the first time in which either $a(T) = -a_{\min,brake}$ or $v(T) = 0$, that is,

$$\begin{aligned} T_1 &= \frac{a_0 + a_{\min,brake}}{j_{\max}} \\ T_2 &= \frac{a_0 + \sqrt{a_0^2 + 2 j_{\max} v_0}}{j_{\max}} \\ T &= \min\{T_1, T_2\} \end{aligned} \tag{5}$$

The lead vehicle travels at speed v_f and decelerates at constant acceleration $a_{max,brake}$; thus, the safe distance formula is:

$$d_{safe} = \left[\left[v_0 T + \frac{1}{2} a_0 T^2 - \frac{1}{6} j_{\max} T^3 \right] + \frac{(v_0 + a_0 T - \frac{1}{2} j_{\max} T^2)^2}{2|a_{\min,brake}|} - \frac{v_f^2}{2|a_{\max,brake}|} \right]_+ \tag{6}$$

The safe distance is calculated based on the velocity and acceleration of the ego car, the velocity of the LV, and three pre-defined parameters: $a_{min,brake}$, j_{max}, and $a_{max,brake}$. The three pre-defined parameters were tested with the approximated 50th, 75th, 95th percentiles of SV maximum deceleration, SV maximum jerk, and LV maximum deceleration shown in Fig. 1. A total of 27 (3 × 3 × 3) APB algorithms were pre-tested in the simulation. The results showed that the algorithm with $a_{min,brake} = 6.7$ m/s^2, $a_{max,brake} = 8.1$ m/s^2, and $j_{max} = 1.7$ g had the least number of crashes;

these parameters were therefore chosen as the APB parameters for further study.

4.4. Improved APB systems

In a previous study (Zhou and Wang, 2022) by the current authors, it was discovered that even though the APB had better driving stability than AEB, it had some safety issues making it unable to prevent all the SCEs from becoming crashes. Specifically, APB does not consider response time, its safe distance fluctuates, and its sensitivity depends on parameter values. To solve these problems, three safety improvement strategies are proposed in the current study. The strategies, which entail modifications to response time, safety buffer, and minimum following distance, are used in different combinations in four APB models that are compared with each other and with the two AEB systems to determine the effectiveness of the strategies.

4.4.1. Response time

The original calculation of APB safe distance does not take the response time of the autonomous vehicle into consideration. Response time (ρ) refers to the time between the start of the unsafe condition and AV brake onset. The response time of the AV applied in existing literature varies between 0.1 s and 0.5 s (Shladover et al., 2015; Li et al, 2016; Li et al, 2017), and the calibrated response time of the RSS model based on car-following SCEs is 0.458 s (Xu et al., 2021). Based on the literature, the AV response time for this improvement to the APB was set as 0.45 s. The modified safe distance equation is shown in Eq. (7), which adds to Eq. (6) the distance that the vehicle travels during the response time, under the assumption that the vehicle keeps its initial acceleration a_0 during that time.

$$d_{safe} = \left[\left[v_0 T + \frac{1}{2}a_0 T^2 - \frac{1}{6}j_{\max} T^3\right] + \frac{\left(v_0 + a_0 T - \frac{1}{2}j_{\max} T^2\right)^2}{2\left|a_{\min,brake}\right|} - \frac{v_f^2}{2\left|a_{\max,brake}\right|} + v_0\rho + \frac{1}{2}a_0\rho^2\right]_+ \tag{7}$$

4.4.1.1. Safety buffer. As is shown in Fig. 5, the safe distance fluctuates frequently with changes in velocity and acceleration. Points A, B and C illustrate one complete cycle of the fluctuation process: 1) at point A, relative distance is smaller than safe distance so the following AV decelerates; 2) this decrease of velocity and acceleration makes it easier for the AV to reach a full stop, thereby reducing the safe distance from point A to B; 3) once the safe distance drops below relative distance at point B, the condition is defined as safe, in which the vehicle will stop the braking process and start to accelerate; 4) at point B, however, it is evident that there is little difference between relative distance and safe distance; thus, at point C, relative distance soon becomes smaller again than safe distance, and the vehicle again begins to decelerate. This fluctuation, which can be seen to recur after point C, may cause the calculated safe distance to be inadequate because part of the distance is eroded by the unanticipated acceleration. Such fluctuation exists in the RSS safe distance as well as in the APB. The essential problem of the safe distance fluctuation is that it causes undesired acceleration during the time and distance that the vehicle should be decelerating.

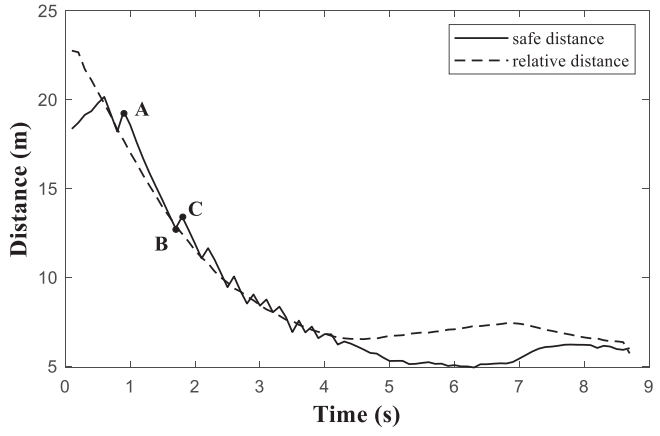

Fig. 5. Safe distance and relative distance of a sample SCE.

Therefore, to reduce the premature acceleration in order to decelerate sufficiently, a modification was made to redefine the safe condition with a stricter criterion. In Eq. (8), we propose a safety buffer, which is the distance that the AV travels in a short period of time at its current velocity v_0. With the buffer, the AV does not accelerate immediately when relative distance is larger than safe distance, but, instead, it keeps decelerating until relative distance is larger than safe distance plus the safety buffer. The safety buffer is designed to be adequate for preventing crashes while not redundant or overly conservative, so values between 0.1 s and 0.5 s were pre-tested: 0.2 s was the lowest value that could prevent crashes.

$$d_{relative} > 0.2 \times v_0 + d_{safe} \tag{8}$$

4.4.1.2. Minimum following distance. The third issue is that APB's calculation of safe distance was less sensitive in low-speed car-following conditions. Supposing that the AV travels at a constant speed of 5 m/s following an LV traveling at the speed of 4 m/s, the AV's brake will not be activated until the relative distance is shorter than 1.82 m. If the AV follows too closely, it will very likely collide with the LV if the LV brakes suddenly. Therefore, the following improvement was made: if the relative distance is shorter than a minimum following distance, $a_{min.brake}$ will be immediately applied without using jerk. The minimum following distance follows the concept of standstill distance, defined as the desired distance between stopped vehicles (Cunto and Saccomanno, 2008). As the standstill distance ranges between 1.0 and 3.0 m in previous studies (Cunto and Saccomanno, 2008; Zhao et al., 2018; Park and Schneeberger, 2003), the default minimum following distance selected in this study was 2.0 m.

Combining the three above strategies by a control variable method, namely adding one strategy each time, four improved (IP) APB systems (IP1-4) were formed. The improved APB systems were then tested and compared with the baseline (BL) APB system, which is the original APB

Table 3
Summary of improved APB systems in this study.

APB system	Response Time	Safety buffer	Minimum following distance
IP1	√		
IP2	√	√	
IP3	√		√
IP4	√	√	√

system with $a_{min,brake} = 6.7$ m/s^2, $a_{max,brake}$=8.1 m/s^2 and $j_{max} = 1.7$ g/s. The improved systems IP1-4 all use the same parameter values as BL, but adopt different strategies (Table 3).

4.5. Evaluation indicators

Evaluation of the autonomous braking systems considers safety, conservativeness, and comfort. Four indicators were used to evaluate safety: number of crashes, minimum TTC, time-integrated time-to collision (TIT), and driving volatility. One indicator was used to evaluate conservativeness: relative distance at the time of brake activation. Two indicators were used to evaluate driving comfort: maximum deceleration and maximum jerk.

4.5.1. Number of crashes

Although one crash actually occurred in the NDS SCEs before extraction, the other crashes were avoided because the drivers successfully performed evasive maneuvers. Number of crashes is therefore an important indicator because an autonomous braking system could still cause a crash in an SCE if the AV did not apply the brake in time or with sufficient strength.

4.5.1.1. Minimum time-to-collision (min TTC). Time-to-collision (TTC) is a widely used indicator of crash risk: a lower TTC represents higher crash risk. Minimum TTC, therefore, can be an intuitive representation of the maximum crash risk in the full car-following period, or event. It is generally considered that a TTC equal or less than 1.5 s would result in an unsafe situation (Morando et al., 2018).

4.5.1.2. Time-integrated time-to-collision (TIT). TTC is only measured at a given instant, so it cannot show how long the risky event lasts nor its severity within a given trip. The TIT indicator, in contrast, uses the integral of the time-to-collision profile of a trip to express the level of safety (in s^2) over a certain time period (Minderhoud and Bovy, 2001). The TIT in a discrete time period is:

$$TIT = \sum_{t=1}^{T} (TTC^* - TTC(t)) \times \tau_{SC} \quad \forall 0 \leqslant TTC(t) \leqslant TTC^* \tag{9}$$

where TIT is the time-integrated TTC over time period T; $TTC(t)$ is the time-to-collision at time t; TTC^* is the TTC evaluation threshold, which is 4 s in this study; and τ_{sc} is the time interval between two simulation steps, which is set at 0.1 s. It is clear that the lower the TIT, the safer is the trip.

4.5.1.3. Driving volatility (V_{dev}). A driver whose speed fluctuates greatly and who brakes sharply will disrupt the stability of his or her immediate traffic environment and increase the likelihood of rear-end collisions. As previous studies have found that driving volatility is significantly correlated with crash frequency (Wali et al., 2018), a braking algorithm that maintains a low level of driving volatility is a vital safety feature for the vehicles surrounding the AV. Measures for driving volatility include standard deviation, coefficient of variation, and mean absolute deviation, all of which can be used to calculate longitudinal speed, acceleration, and jerk (Kamrani et al., 2018). In this study, standard deviation of speed is used for measuring driving volatility as it is simple and intuitive:

$$V_{dev} = \sqrt{\frac{1}{T-1} \sum_{t=1}^{T} (v_t - \bar{v})^2} \tag{10}$$

where V_{dev} is the standard deviation of speed over time period T; v_t is the vehicle speed at time t; and $\bar{v}$ is the mean speed over time period T.

4.5.1.4. Relative distance when the brake is activated (Dis_a). A large relative distance at brake activation time implies that the system is very conservative, and may disturb drivers and waste road resources. A system that is more efficient and can still ensure safety is preferred.

4.5.1.5. Maximum deceleration and maximum jerk. Because AVs respond faster and have better control capability than human drivers, their rapid and strong maneuvers produce jerk and other forces that act on drivers and passengers, and are likely to lead to discomfort (Elbanhawi et al., 2015). Acceleration, either positive or negative, as well as jerk, are easily accessed kinetic parameters that can be used to measure passenger comfort (Martin and Litwhiler, 2008). They have thus been included in vehicle system development and assessment in the comfortable navigation framework proposed by Morales et al. (2013) and the comfort index proposed by Kosaki et al. (2021). As maximum deceleration and maximum jerk are two key parameters in the braking process, they were selected as indicators to evaluate driving comfort.

5. Results

5.1. Evaluation of the APB systems and AEB systems

The overall performance of the baseline and four improved APB systems were evaluated along with the one-stage and three-stage AEB systems. Using the seven evaluation indicators in Section 4.5, their performance was compared with the performance of SH-NDS human drivers.

Fig. 6 shows the number of crashes in the simulation for each system. With 108 crashes, the BL failed to defuse risk in 48 % (108/223) of SCEs. The improved APB sytems, IP1-4, all considered response time in the safe distance calculation. This was the only modification in IP1, and it prevented 25 more crashes from occurring. IP2 added a safety buffer to the distance criterion, whereby 22 additional crashes were prevented. The minimum following distance limitation was demonstrated to be even more effective, as IP3, which included this modification but not the safety buffer, prevented 75 more crashes than IP1, leaving only 8 crashes. Combining all three strategies, IP4 succeeded in preventing all crashes, thus outperforming all studied sytems, including the two AEB systems. IP4 also managed to prevent the single human driver crash.

Based on the other three safety indicators, the four improved APB systems (IP1-IP4) had overall better safety performance than the BL. As is shown in Fig. 7a and 7b, IP1-IP4 have higher minimum TTC and lower TIT than BL, with IP4 outperforming all the APB systems. Though IP4 had slightly greater driving volatility (V_{dev}) than the other APB systems (Fig. 7c), its overall ability, and especially its ability to prevent crashes, far exceeded that of the others. IP4, additionally, had lower volatility than the AEB systems; indeed, all improved APB systems show better safety performance than the AEB systems with their significantly larger minimum TTC, lower TIT and lower volatility. By all measures but TTC, however, the safety performance of BL was worse than that of the two AEB systems, confirming the results of Zhou and Wang (2022). IP4 outperformed human drivers overall as it generated larger average minimum TTC (2.99 s against 1.31 s), achieved lower driving volatility (2.66 m/s against 3.30 m/s), and prevented the single crash in the extracted SCEs.

Conservativeness was measured by relative distance at the time of brake activation (Dis_a). Fig. 7d shows that the four improved APB systems have larger brake activation distance, and therefore brake earlier, than BL. This increase in conservativeness is a result of adding response time to the safe distance functions of IP1-IP4. All the APB systems, however, are slightly more conservative than the AEB systems, but this is counterbalanced by their safety: while IP4 prevented all crashes, the AEB systems failed to prevent many of the crashes because they were activated too late. IP4 is also less conservative than human drivers, as the mean Dis_a of IP4 (9.63 m) is shorter than that of the human driver

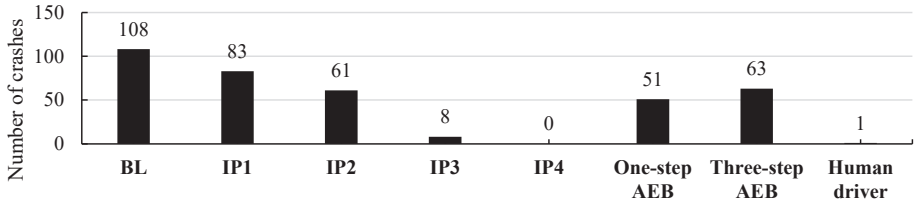

Fig. 6. Number of crashes under the control of baseline and improved APB systems, one-step and three-step AEB systems, and human drivers.

(11.90 m).

Evaluation of the systems by the two comfort indicators, maximum deceleration and maximum jerk, are shown in Fig. 7e and 7f. The lower boundaries of the maximum deceleration are around -6.6 m/s^2 as BL and IP1-4 share the same minimum reasonable braking value $a_{min,brake}$ of 6.7 m/s^2. However, though j_{max} in the five APB systems are all 1.7 g/s, the maximum jerk in IP3 and IP4 are significantly larger than in BL, IP1 and IP2, which is caused by the application of the minimum following distance strategy. When the relative distance is smaller than minimum following distance, $a_{min,brake}$ will be applied directly without using the jerk-bounded profile to achieve an emergency brake; the actual jerk of this brake will be large. The mean maximum deceleration (-7.456 m/s^2) and mean maximum jerk (7.309 g/s) of one-stage AEB are significantly larger than that of the other systems, which indicate the one-stage hard brake has the poorest driving comfort, and is likely beyond passengers' tolerence. Although IP4 achieved satisfactory safety performance without being overly conservative, its overall driving comfort is inferior to that of BL, IP1, IP2, and human drivers because, to perform a rapid brake in low-speed car-following, it uses the minimum following distance strategy that abandons the more comfortable jerk-bounded braking profile.

5.2. *Examples of the improvements to the APB systems safe distance trigger*

By means of the seven indicators, the overall performance of the improved APB systems has been evaluated, but the underlying mechanisms of the safety improvement strategies are not fully revealed. Each of the strategies has specific effects on safe distance that varies according to the AV's velocity and acceleration at each simulation step, therefore, safe distance will be analyzed in this section to reveal the improvement of each strategy.

As discussed in Section 4.4 and shown in Table 3, the improved APB systems were designed with control variables so that the individual effectiveness of each of the three strategies could be evaluated. By comparing BL with IP1, the effect of Strategy 1, response time, can be revealed. Similarly, the effect of Strategy 2, the safety buffer, can be revealed by comparing IP1 with IP2, and IP3 with IP4; the effect of Strategy 3, minimum following distance, can be revealed by comparing IP1 with IP3, and IP2 with IP4. To illustrate the specific effects of the strategies, three events were selected that most clearly demonstrate their effectiveness. That is, in each of these events, the application of a particular strategy prevented crashes, while crashes occurred with the APB systems that did not use the strategy. Fig. 8 shows the safe distance curves and the resulting relative distance curves of the three events, with the strategies they illustrate, plotted for each of the five APB systems. Where a curve stops before the end of the event, that system has caused a crash.

The curves in Fig. 8a illustrate the impact of the first strategy, response time, on the safe distance in Event 1. As noted earlier, the BL system does not consider the distance that the vehicle travels during response time, so BL's safe distance is significantly shorter than that of the four improved systems IP1-IP4 due to their added response time. The omission of response time was the main reason for the large number of BL crashes (108, shown in Fig. 6). As can be seen in Fig. 8b, BL caused a crash at around 7.5 s due to the small calculated safe distance.

Event 2 illustrates the second strategy, used in IP2 and IP4, which was to reduce excessive safe distance fluctuation by modifying acceleration activation logic and using a safety buffer. This strategy thereby avoids premature resumption of acceleration, giving the AV the time to decelerate and thus keep an adequate relative distance to the LV. In Fig. 8c, the decrease of safe distance results from the vehicle decelerating, while the sharp increase of the curves means the safe distance has become shorter than relative distance, and so the vehicle starts to accelerate. Comparing IP3 and IP4 in the first 4 s, the safe distance fluctuation range of IP3 is smaller than that of IP4 but the time between fluctuations is greater for IP4; that is, IP4 fluctuated less frequently than IP3, meaning that the undesirable acceleration appears less often. This allowed the vehicle to decelerate for a longer time, which made the relative distance between the two vehicles larger, as shown in Fig. 8d. This longer period of deceleration is the reason that, with the application of the safety buffer, safety can be somewhat improved.

Event 3 illustrates the strategy that establishes a minimum following distance. In this event, the AV braked early, and its speed was low at around 5 to 6 s. The calculated safe distance (Fig. 8e) is small when the speed is low, even reaching zero at around 5.5 s, 9 s, and 13 s, in each case being lower than the relative distance (Fig. 8f). In such cases, even if the two vehicles are very close to each other, the brake may not be triggered in time. Thus, it can be seen in Event 3 that BL crashed at the 5th second, followed by IP1 and IP2, which failed to prevent the crash at about the 8th second. IP3 and IP4 applied the minimum relative distance limitation at about 6 s, 9 s, and 12 s, where the car decelerated and the safe distance suddenly decreased, thus preventing the crash. The example of Event 3 demonstrates that establishing a minimum relative distance is effective in low-speed following conditions.

In conclusion, these three typical events demonstrate the mechanisms underlying the three safety improvement strategies. Considering the response time in the safe distance equation will increase the value of safe distance and thereby activate the brake earlier with adequate braking distance. The safety buffer can extend the deceleration time and keep the AV much further from the lead vehicle. The minimum relative distance limitation is effective when the AV is at a low speed and the relative distance between the two vehicles is small. By taking advantage of all three strategies, all crashes in this study were successfully prevented.

6. Discussion

Three safety improvement strategies were proposed for APB system in this study, they are: 1) adding a response time of 0.45 s in APB's safe distance equation, 2) using a safety buffer, and 3) using a minimum following distance limitation. All three of the strategies were demonstrated to be effective in improving APB's safety performance. Together, they advanced the brake activation time, reduced premature acceleration, and activated, even at low speeds, at a 2-m minimum following distance. As each of the strategies has its own specific effect that can avoid a certain kind of crashes, applying one or two of the strategies cannot avoid the crashes that should be dealt with the strategies not included in the system. IP4, the improved system that adopted all three strategies, outperformed the BL, the other three improved APB systems,

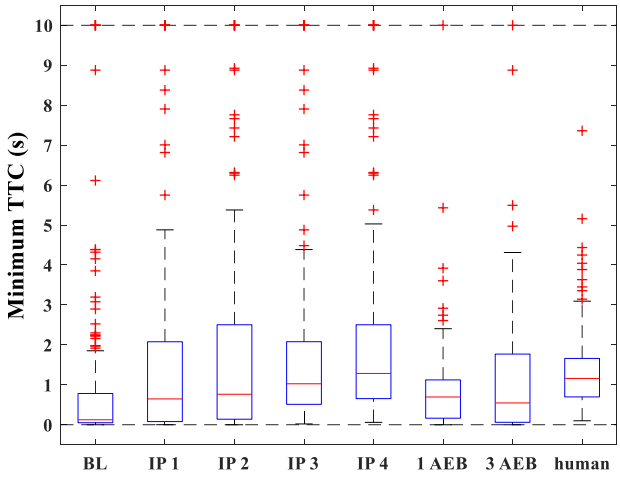

(a) Minimum TTC

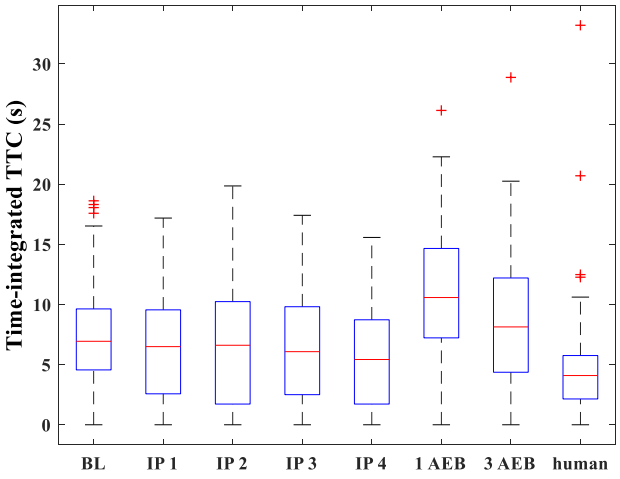

(b) TIT

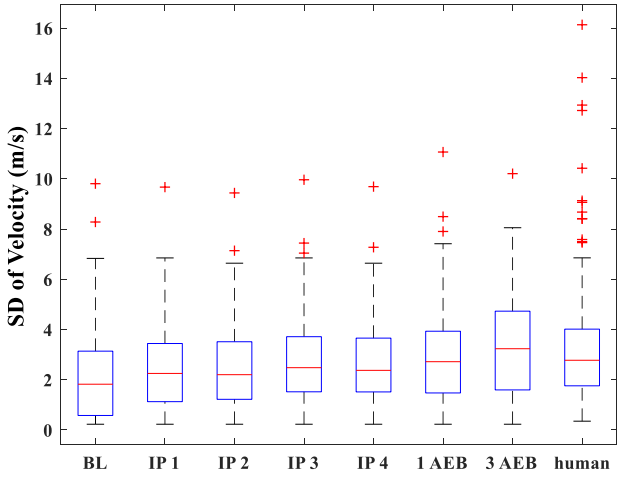

(c) Standard Deviation of Velocity

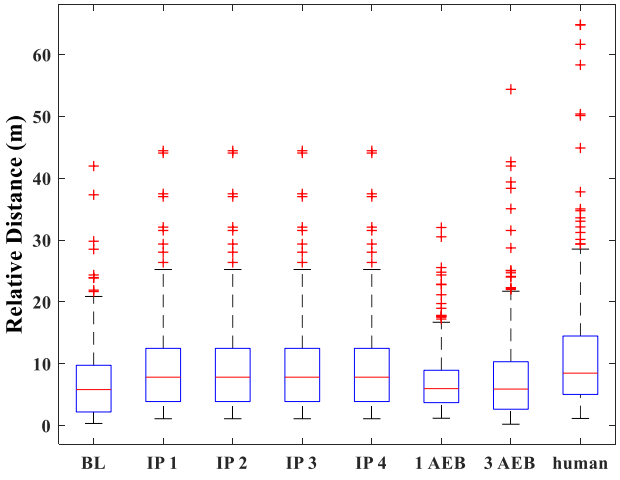

(d) Relative Distance at Brake Activation

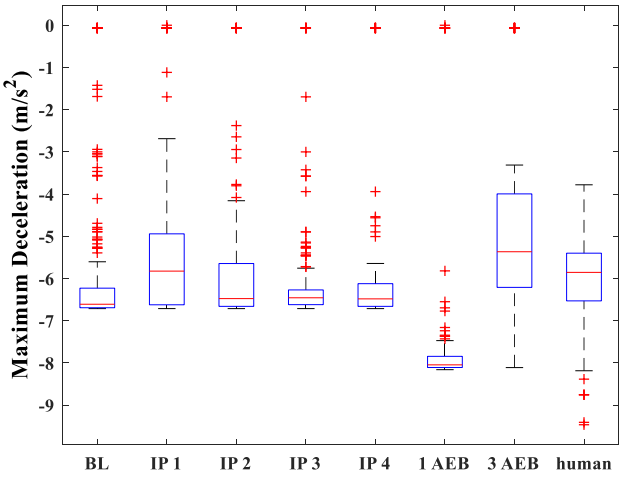

(e) Maximum Deceleration of Ego Vehicle

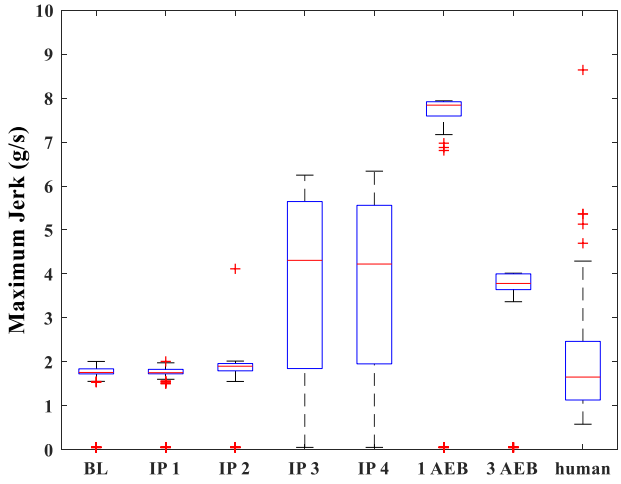

(f) Maximum Jerk of Ego Vehicle

Fig. 7. Minimum TTC, TIT, SD of velocity, and relative distance at brake activation time for APB systems, AEB systems, and human drivers.

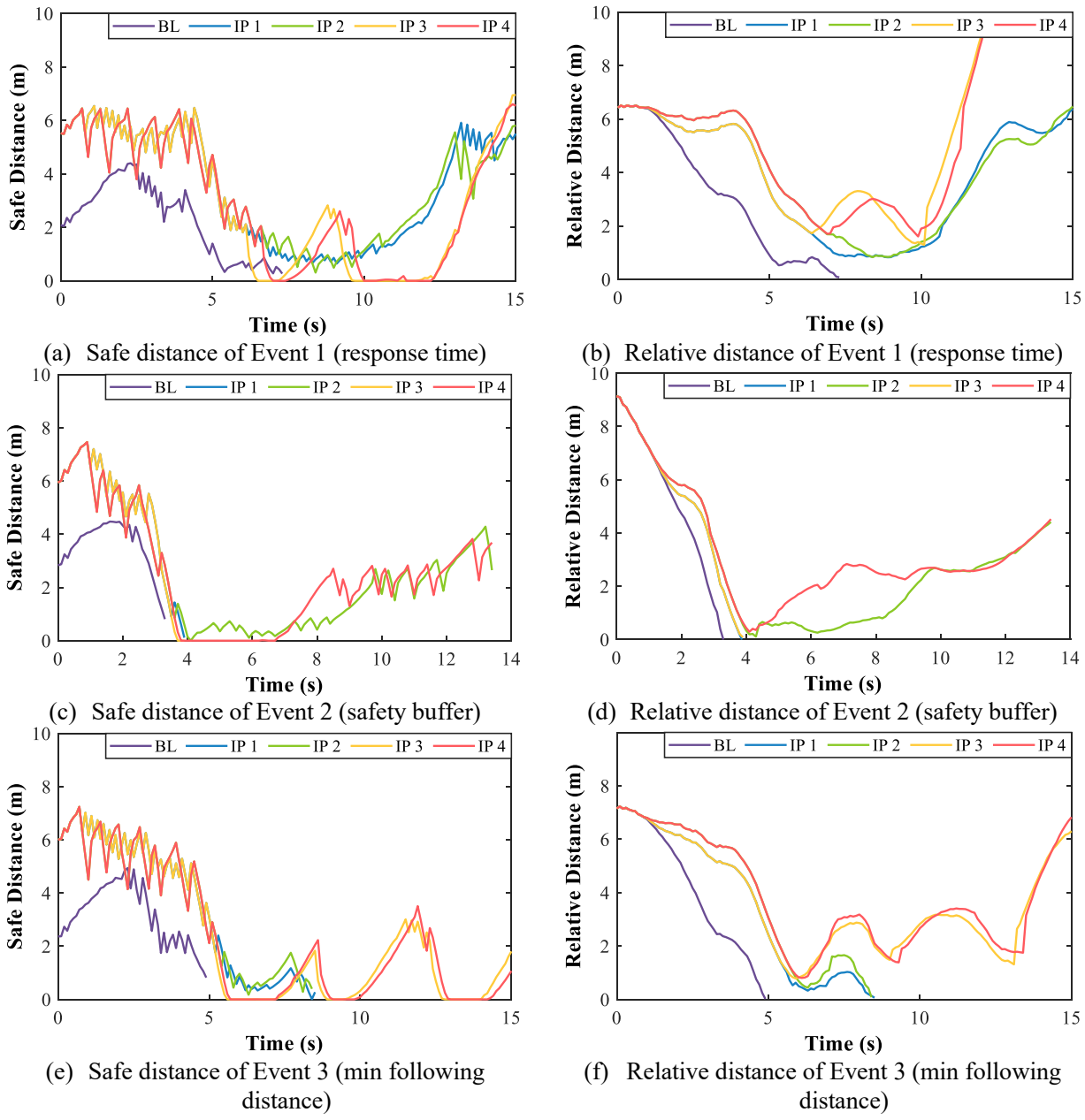

Fig. 8. Safe distance of the five APB systems in three sample events.

and the two AEB systems in safety performance.

Adding response time into APB's safe distance calculation increased its conservativeness, but the improved APB is still more efficient than both RSS and human drivers. A similar study of car-following events showed RSS's conservativeness in its activating the brake 2.31 s earlier than human drivers (Xu et al., 2021), thereby keeping a longer car-following distance. In the current study, IP4 braked 1.13 s later than human drivers, with its average brake activation distance 2.27 m shorter than that of human drivers. APB is less conservative than RSS because APB uses the AV's real-time acceleration during response time, while RSS uses the maximum AV acceleration in any condition. This explanation is consistent with the findings of Mattas (2020) that RSS's use of the maximum AV acceleration in any condition was the reason for RSS's high false positive rate, that is, RSS's triggering of the brake when it was unnecessary. One way that has been found to reduce the false positive rate is to take the drivers' reaction into consideration and trigger the brake only if the driver has already applied the brake in an emergency manner (Hillenbrand et al., 2005). The current study showed that IP4 braked later than human drivers on average, indicating it should lead to a lower false alarm rate. However, one limitation of this study is that because the systems were tested only with SCEs, the intervention of the collision avoidance system was never unnecessary; that is, there were no normal car-following scenarios in which braking interventions could be considered false positives.

This study's findings demonstrated that jerk-bounded braking is able to improve driving comfort. One-stage AEB, which directly applies a constant hard brake, showed the poorest driving comfort, and the comfort of the APB system was sacrificed for better safety performance when the minimum following distance strategy was applied to IP3 and IP4. IP3 and IP4 abandon APB's jerk-bounded braking when the 2-m minimum following distance is met, and instead apply a rapid brake at an imminent crash. In close and critical car-following scenarios these two systems brake like AEB, which, though less comfortable, caused the crash number to decrease greatly. This finding implies that different

braking patterns can be conditionally integrated to improve APB's overall performance.

The difference between AEB and APB is how they balance between brake activation time and braking force, which affects efficiency and driving comfort, and more importantly, safety. AEB uses a hard and late brake in order to prevent a crash or mitigate its severity without incurring false alarms, while APB adopts a milder and more proactive brake. The two AEB systems, both with a highest deceleration of 8.1 m/s^2, failed to prevent SCEs from deteriorating into crashes in 22.87 % and 28.25 % of the events, respectively. This deceleration is similar to that of Mazda's collision avoidance system (8 m/s^2) (Lee and Peng, 2005), but not as high as the 10 m/s^2 deceleration of Volvo S60 (Coelingh et al., 2010) and Mercedes CLS (ADAC, 2013). In this study, 8.1 m/s^2 was the highest maximum deceleration, the 95th percentile of SV driver in the NDS: a higher deceleration is seldomly used by drivers. A higher deceleration may theoretically reduce the crash rate, but, as the system's efficiency relies on the balance between brake activation time and braking force, brake activation may be delayed, resulting in lower safety in actual practice. The improved APB systems have been demonstrated to be more conservative than either of the AEB systems based on the longer relative distance that they require for brake activation, as well as on their milder maximum deceleration rate (6.7 m/s^2). Considering that an AV's unexpected hard brake could cause a following conventional vehicle, driven by a human driver with little time to react, to hit the AV from behind (Liu et al., 2021a, Liu et al., 2021b), this conservativeness implies that APB has the potential of protecting the AV from being rear-ended.

7. Conclusion

To explore ways to ensure the traffic safety of AVs in car-following scenarios, especially to reduce the risk of the AV colliding with the lead vehicle, three safety improvement strategies for APB system were proposed. The strategies were used in different combinations in four improved APB systems (IP1-IP4) and compared with the baseline APB (BL), as well as with two AEB systems: one-stage AEB and three-stage AEB. A total of 223 car-following SCEs (including one crash) were extracted from the Shanghai Naturalistic Driving Study and recreated in the MATLAB simulation platform. An AV controlled by these seven autonomous braking systems replaced the human-driven subject vehicle in the virtual scenarios built according to the trajectory and velocity of the lead vehicle in the SCEs. Using the simulated SCEs, the systems' safety performance, conservativeness, and driving comfort were evaluated and compared with each other and with the NDS human drivers. The major findings are summarized below:

1) all the three proposed strategies were demonstrated to be effective in improving APB system's safety performance. IP4, the system that integrated all three strategies, outperformed the baseline APB and IP1-IP3 and prevented all SCEs from becoming crashes;
2) IP4 was slightly more conservative than AEB due to the application of response time strategy, but was less conservative than RSS;
3) APB's jerk-bounded braking profile is able to improve driving comfort;
4) though the two AEB systems applied higher deceleration than in IP4, they failed to prevent all crashes.

The study still has some limitations. While the safety focus of this study has been on preventing collision with the AV's lead vehicle, it can be deduced that our improvements to APB's deceleration and jerk should also help the interaction between the AV and its following vehicle, but the performance of the following vehicle was not verified. Future research using a driving simulator, as Wang et al. (2016) used to study drivers' collision avoidance behavior in urgent situations, can consider drivers' reaction time, brake reaction, and stopping distance to further explore the response of a human-driven vehicle following an APB-equipped AV to determine whether the milder braking of APB can mitigate AVs being hit from behind. Another limitation is that the false positive rate of the systems cannot be tested as only SCEs are simulated. Safe car-following events can be further studied to test the false positive rates of the systems.

The main contribution of the study is the development of an improved APB system, IP4, which has been shown in this study to provide safer and milder, that is, more conservative and more comfortable, braking for AVs in car-following SCEs than AEB systems, while avoiding the over-conservativeness of RSS. An important end goal in AV research is to develop AV systems that can be well understood by surrounding vehicles and enable the AV to better cooperate with other road users. Conditional upon further simulator and field testing to determine any other needed modifications, the system has the potential to be applied in vehicle collision avoidance systems as a safer and more stable alternative to AEB.

Declaration of Competing Interest

The authors declare that they have no known competing financial interests or personal relationships that could have appeared to influence the work reported in this paper.

Data availability

The data that has been used is confidential.

Acknowledgments

This study was jointly sponsored by the Chinese National Science Foundation (51878498) and the Science and Technology Commission of Shanghai Municipality (18DZ1200200). The authors appreciate Barbara Rau Kyle for her helpful revision and polish.

Author contributions

The authors confirm their contribution to the paper as follows: study conception and design: Weixuan Zhou, Xuesong Wang, Xiangbin Wu; data preparation: Xiaoyan Xu, Weixuan Zhou; analysis and interpretation of results: Weixuan Zhou; draft manuscript preparation: Weixuan Zhou, Yi Glaser. All authors reviewed the results and approved the final version of the manuscript.

References

Allgemeiner Deutscher Automobil-Club (ADAC), 2013. Comparative Test of Advanced Emergency Braking Systems.

Brannstrom, M., Sjoberg, J., Coelingh, E., 2008. A situation and threat assessment algorithm for a rear-end collision avoidance system. Proceedings of 2008 IEEE Intelligent Vehicles Symposium.

Burgett, A., Carter, A., Preziotti, G., 2001. An algorithm for rear-end collision avoidance warning systems. In: 17th International Technical Conference on the Enhanced Safety of Vehicles, pp. 4–7.

Carney, C., McGehee, D.V., Lee, J.D., Reyes, M.L., Raby, M., 2010. Using an event-triggered video intervention system to expand the supervised learning of newly licensed adolescent drivers. Am. J. Public Health 100 (6), 1101–1106.

Char, F., Serre, T., Compigne, S., Puente Guillen, P., 2022. Car-to-cyclist forward collision warning effectiveness evaluation: a parametric analysis on reconstructed real accident cases. Int. J. Crashworthiness 27 (1), 34–43.

Chen, Y.L., Shen, K.Y., Wang, S.C., 2013. Forward collision warning system considering both time-to-collision and safety braking distance. IJVS 6 (4), 347.

Cicchino, J.B., 2016. Effectiveness of forward collision warning and autonomous emergency braking systems in reducing front-to-rear crash rates. Accid. Anal. Prev. 99, 142–152.

Coelingh, E., Eidehall, A., Bengtsson, M., 2010. Collision warning with full auto brake and pedestrian detection - a practical example of automatic emergency braking. Proceedings of 13th International IEEE Conference on Intelligent Transportation Systems.

Cunto, F., Saccomanno, F.F., 2008. Calibration and validation of simulated vehicle safety performance at signalized intersections. Accid. Anal. Prev. 40 (3), 1171–1179.

Dingus, T.A., Klauer, S.G., Neale, V.L., Petersen, A., Lee, S.E., Sudweeks, J., et al., 2006. The 100-Car Naturalistic Driving Study Phase II – Results of the 100-Car Field

Experiment. Publication No. DOT-HS-810-593. U.S. Department of Transportation, National Highway Traffic Safety Administration.
Doecke, S.D., Anderson, R.W.G., Mackenzie, J., Ponte, G., 2012. The Potential of Autonomous Emergency Braking Systems to Mitigate Passenger Vehicle Crashes. Proceedings of Australasian Road Safety Research, Policing and Education Conference.
Doi, A., Butsuen, T., Niibe, T., Takagi, T., Yamamoto, Y., Seni, H., 1994. Development of a Rear-end Collision Avoidance System with Automatic Brake Control. Jsae Review 15 (4), 335–340.
Elbanhawi, M., Simic, M., Jazar, R., 2015. In the passenger seat: investigating ride comfort measures in autonomous cars. IEEE Intell. Transp. Syst. Mag. 7 (3), 4–17.
Fildes, B., Keall, M., Bos, N., Lie, A., Page, Y., Pastor, C., Pennisi, L., Rizzi, M., Thomas, P., Tingvall, C., 2015. Effectiveness of low speed autonomous emergency braking in real-world rear-end crashes. Accid. Anal. Prev. 81, 24–29.
Fujita, Y., Akuzawa, K., Sato, M., 1995. Radar Brake System. Jsae Rev. 1 (16), 113.
Gassmann. B., Oboril, F., Buerkle, C., Liu, S., Yan, S., Elli, M.S., Alvarez, I., Aerrabotu, N., Jaber, S., Van Beek, P., Iyer, D., Weast, J., 2019.et al. Towards Standardization of AV Safety: C++ Library for Responsibility Sensitive Safety. Proceedings of IEEE Intelligent Vehicles Symposium (IV).
Gettman, D., Pu, L., Sayed, T., Shelby, S. G., Energy, S., 2008. Surrogate Safety Assessment Model and Validation, Publication No. FHWA-HRT-08-051. Turner-Fairbank Highway Research Center.
Guo, F., 2019. Statistical methods for naturalistic driving studies. Annu. Rev. Stat. Appl. 6 (1), 309–328.
Guo, F., Klauer, S.G., Hankey, J.M., Dingus, T.A., 2010. Near crashes as crash surrogate for naturalistic driving studies. Transp. Res. Rec. 2147 (1), 66–74.
Hankey, J.M., Perez, M.A., McClafferty, J.A., 2016. Description of the SHRP 2 Naturalistic Database and the Crash, Near-Crash, and Baseline Data Sets. Virginia Tech Transportation Institute.
Hillenbrand, J., Kroschel, K., Schmid, V., 2005. Situation assessment algorithm for a collision prevention assistant. In: IEEE Proceedings. Intelligent Vehicles Symposium, pp. 459–465.
Hogema, J. H., & Janssen, W. H. 1996. Effects of intelligent cruise control on driving behaviour: a simulator study. In Intelligent Transportation: Realizing the Future. Abstracts of the Third World Congress on Intelligent Transport Systems.
Hirst, S., Graham, R., 1997. The format and presentation of collision warnings. In: Ergonomics and safety of intelligent driver interfaces. CRC Press, pp. 203–219.
Jeppsson, H., Lubbe, N., 2020. Simulating Automated Emergency Braking with and without Torricelli Vacuum Emergency Braking for Cyclists: Effect of Brake Deceleration and Sensor Field-of-view on Accidents, Injuries and Fatalities. Accid. Anal. Prev. 142, 1–15.
Kamrani, M., Arvin, R., Khattak, A.J., 2018. Extracting useful information from basic safety message data: an empirical study of driving volatility measures and crash frequency at intersections. Transp. Res. Rec. 2672 (38), 290–301.
Koopman, P., Osyk, B., 2019. Autonomous Vehicles Meet the Physical World: RSS, Variability, Uncertainty, and Proving Safety. arXiv:1911.01207.
Kosaki, S., Ejiri, A., Oya, M., 2021. Development of driver braking control model based on ride comfort index. Artificial Life Robotics 26 (3), 347–353.
Kusano, K.D., Gabler, H.C., 2012. Safety benefits of forward collision warning, brake assist, and autonomous braking systems in rear-end collisions. Proc. IEEE Trans. Intell. Transport. Syst. 13 (4), 1546–1555.
Lee, D.H., Kim, S.K., Kim, C.S., Huh, K.S., 2014. Development of an autonomous braking system using the predicted stopping distance. Int. J. Automot. Technol. 15 (2), 341–346.
Lee, K., Peng, H., 2005. Evaluation of automotive forward collision warning and collision avoidance algorithms. Veh. Syst. Dyn. 43 (10), 735–751.
Lee, S.E., Simons-Morton, B.G., Klauer, S.E., Ouimet, M.C., Dingus, T.A., 2011. Naturalistic Assessment of Novice Teenage Crash Experience. Accid. Anal. Prev. 43, 1472–1479.
Li, L., Peng, X., Wang, F.Y., Cao, D., Li, L., 2018. A situation-aware collision avoidance strategy for car-following. Proc. IEEE/CAA J. Autom. Sin. 5 (5), 1012–1016.
Li, Y., Wang, H., Wang, W., Liu, S., Xiang, Y., 2016. Reducing the risk of rear-end collisions with infrastructure-to-vehicle (I2V) integration of variable speed limit control and adaptive cruise control system. Traffic Inj. Prev. 17, 597–603.
Li, Y., Wang, H., Wang, W., Xing, L., Liu, S., Wei, X., 2017. Evaluation of the impacts of cooperative adaptive cruise control on reducing rear-end collision risks on freeways. Accid. Anal. Prev. 98, 87–95.
Liu, Q., Wang, X., Wu, X., Glaser, Y., He, L., 2021a. Crash comparison of autonomous and conventional vehicles using pre-crash scenario typology. Accid. Anal. Prev. 159, 2–13.
Liu, S., Wang, X., Hassanin, O., Xu, X., Yang, M., Hurwitz, D., Wu, X., 2021b. Calibration and evaluation of responsibility-sensitive safety (RSS) in automated vehicle performance during cut-in scenarios. Transport. Res. Part C: Emerg. Technol. 125, 1–15.
Martin, D., Litwhiler, D., 2008. An investigation of acceleration and jerk profiles of public transportation vehicles. Proceedings of 2008 Annual Conference & Exposition.
Mattas, K., Makridis, M., Botzoris, G., Kriston, A., Minarini, F., Papadopoulos, B., Re, F., Rognelund, G., Ciuffo, B., 2020. Fuzzy Surrogate Safety Metrics for Real-time Assessment of Rear-end Collision Risk. A Study Based on Empirical Observations. Accid. Anal. Prev. 148, 1–10.
Minderhoud, M.M., Bovy, P.H.L., 2001. Extended Time-to-collision Measures for Road Traffic Safety Assessment. Accid. Anal. Prev. 33, 89–97.
Mobileye, 2010. Mobileye C2-270 Collision Prevention System User Manual.
Morales, Y., Kallakuri, N., Shinozawa, K., Miyashita, T., Hagita, N., 2013. Human-comfortable Navigation for an Autonomous Robotic Wheelchair. Proceedings of 2013 IEEE/RSJ International Conference on Intelligent Robots and Systems.
Morando, M.M., Tian, Q., Truong, L.T., Vu, H.L., 2018. Studying the safety impact of autonomous vehicles using simulation-based surrogate safety measures. J. Adv. Transport. 2018, 1–11.
NHTSA, 2014. Automatic Emergency Braking System (AEB) Research Report. U.S. Department of Transportation. Available: https://www.automotivesafetycouncil.org/wp-content/uploads/2017/01/NHTSA-AEB-Report.pdf.
Park, M.K., Lee, S.Y., Kwon, C.K., Kim, S.W., 2017. Design of pedestrian target selection with funnel map for pedestrian AEB system. IEEE Trans. Veh. Technol. 66 (5), 3597–3609.
Park, B., Schneeberger, J.D., 2003. Microscopic simulation model calibration and validation: case study of VISSIM simulation model for a coordinated actuated signal system. Transp. Res. Rec. 1856 (1), 185–192.
Perez, M.A., Sudweeks, J.D., Sears, E., Antin, J., Lee, S., Hankey, J.M., Dingus, T.A., 2017. Performance of basic kinematic thresholds in the identification of crash and near-crash events within naturalistic driving data. Accid. Anal. Prev. 103, 10–19.
Seiler, P., Song, B., Hedrick, J.K., 1998. Development of a Collision Avoidance System. SAE Trans. 1334–1340.
Shalev-Shwartz, S., Shammah, S., Shashua, A., 2017. On a Formal Model of Safe and Scalable Self-Driving Cars. arXiv preprint arXiv:1708.06374.
Shalev-Shwartz, S., Shammah, S., Shashua, A., 2018. Vision Zero: Can Roadway Accidents Be Eliminated without Compromising Traffic Throughput? arXiv preprint arXiv: 1901.05022.
Shladover, S.E., Nowakowski, C., Lu, X., Ferlis, R., 2015. Cooperative adaptive cruise control: definitions and operating concepts. Transp. Res. Rec. 2489, 145–152.
Treiber, M., Hennecke, A., Helbing, D., 2000. Congested traffic states in empirical observations and microscopic simulations. Phys. Rev. E 62 (2), 1805.
Wali, B., Khattak, A.J., Bozdogan, H., Kamrani, M., 2018. How is driving volatility related to intersection safety? A Bayesian heterogeneity-based analysis of instrumented vehicles data. Transport. Res. Part C: Emerg. Technol. 92, 504–524.
Wang, X., Xu, X., 2019. Assessing the relationship between self-reported driving behaviors and driver risk using a naturalistic driving study. Accid. Anal. Prev. 128, 8–16.
Wang, X., Zhu, M., Chen, M., Tremont, P., 2016. Drivers' rear end collision avoidance behaviors under different levels of situational urgency. Transport. Res. Part C:Emerg. Technol. 71, 419–433.
Wu, K.F., Jovanis, P.P., 2012. Crashes and crash-surrogate events: exploratory modeling with naturalistic driving data. Accid. Anal. Prev. 45, 507–516.
Xu, C., Ding, Z., Wang, C., Li, Z., 2019. Statistical analysis of the patterns and characteristics of connected and autonomous vehicle involved crashes. J. Saf. Res. 71, 41–47.
Xu, X., Wang, X., Wu, X., Hassanin, O., Chai, C., 2021. Calibration and evaluation of the responsibility-sensitive safety model of autonomous car-following maneuvers using naturalistic driving study data. Transport. Res. Part C: Emerg. Technol. 123, 1–17.
Yang, L., Yang, Y., Wu, G., Zhao, X., Fang, S., Liao, X., Wang, R., Zhang, M., 2022. A systematic review of autonomous emergency braking system: impact factor, technology, and performance evaluation. J. Adv. Transport.
Zhang, T., Gao, K., 2020. Will autonomous vehicles improve traffic efficiency and safety in urban road bottlenecks? the penetration rate matters. Proceedings of IEEE 5th International Conference on Intelligent Transportation Engineering (ICITE).
Zhao, C., Xing, Y., Li, Z., Li, L., Wang, X., 2019. A Right-of-way Assignment Strategy to Ensure Traffic Safety and Efficiency in Lane Change. arXiv preprint arXiv: 1904.06500.
Zhao, L., Malikopoulos, A., Rios-Torres, J., 2018. Optimal control of connected and automated vehicles at roundabouts: An investigation in a mixed-traffic environment. IFAC-PapersOnLine 51 (9), 73–78.
Zhou, W., Wang, X., 2022. Calibrating and comparing autonomous braking systems in motorized-to-non-motorized-vehicle conflict scenarios. IEEE Trans. Intell. Transp. Syst.